



A dual fluorinated and iodinated radiotracer for PET and SPECT imaging of β -amyloid plaques in the brain

Hiroyuki Watanabe^{a,b}, Masahiro Ono^{a,b,*}, Hiroyuki Kimura^a, Shinya Kagawa^c, Ryuichi Nishii^c, Takeshi Fuchigami^b, Mamoru Haratake^b, Morio Nakayama^{b,*}, Hideo Saji^a

^a Department of Patho-Functional Bioanalysis, Graduate School of Pharmaceutical Sciences, Kyoto University, 46-29 Yoshida Shimoadachi-cho, Sakyo-ku, Kyoto 606-8501, Japan

^b Department of Hygienic Chemistry, Graduate School of Biomedical Sciences, Nagasaki University, 1-14 Bunkyo-machi, Nagasaki 852-8521, Japan

^c Shiga Medical Center Research Institute, 5-4-30 Moriyama, Moriyama City, Shiga 524-8524, Japan

ARTICLE INFO

Article history:

Received 31 May 2011

Revised 12 August 2011

Accepted 13 August 2011

Available online 24 August 2011

Keywords:

Alzheimer's disease

β -Amyloid peptide

PET

SPECT

Dual imaging

ABSTRACT

We report a fluorinated and iodinated radiotracer as a probe for PET/SPECT to detect of β -amyloid ($A\beta$) plaques in the brain of patients with Alzheimer's disease (AD). We successfully designed and synthesized the fluorinated and iodinated aurone derivative (**3**) and its radiolabels ($[^{125}I]\mathbf{3}$ and $[^{18}F]\mathbf{3}$). In binding experiments *in vitro*, **3** showed high affinity for $A\beta$ aggregates ($K_i = 6.81$ nM). In brain sections of AD model mice, **3** intensely stained $A\beta$ plaques. Furthermore, a specific plaque labeling signal was observed on the autoradiography of postmortem AD brain sections using $[^{125}I]\mathbf{3}$. In biodistribution experiments using normal mice, $[^{125}I]\mathbf{3}$ and $[^{18}F]\mathbf{3}$ displayed good uptake into and a rapid washout from the brain, properties highly desirable for $A\beta$ imaging agents. These results suggest that **3** may function as a PET/SPECT dual imaging agent for detecting $A\beta$ plaques in AD brains.

© 2011 Elsevier Ltd. All rights reserved.

Alzheimer's disease (AD) is a progressive neurodegenerative disorder characterized by cognitive decline, irreversible memory loss, disorientation, and language impairment. Senile plaques containing β -amyloid ($A\beta$) peptides and neurofibrillary tangles in post-mortem brain are two pathological hallmarks of AD.^{1,2} Excessive production of $A\beta$ via various normal or abnormal mechanisms is considered to be the initial neurodegenerative event in AD. Currently, it is difficult for clinicians to differentiate between the cognitive decline associated with normal aging and the cognitive decline associated with AD. There is no simple and definitive diagnostic method to detect $A\beta$ plaques in the brain without postmortem pathological staining of brain tissue. Thus, the development of imaging agents for positron emission tomography (PET) or single photon emission computed tomography (SPECT), which can detect $A\beta$ plaques *in vivo* may assist with the early diagnosis of AD.^{3–5}

The nuclear imaging modality of choice in the clinic is often PET rather than SPECT in part because of superior sensitivity, resolution, and quantitative ability. Therefore, in the past few years, several groups' efforts have focused on the development of potential PET probes for the detection of $A\beta$ plaques *in vivo*. As a result, PET probes such as $[^{18}F]AV-45$,^{6,7}

$[^{18}F]GE-068$,⁸ $[^{18}F]BAY94-9172$,^{9,10} $[^{11}C]AZD2184$,^{11,12} $[^{11}C]PIB$,^{13,14} $[^{11}C]SB-13$,^{15,16} and $[^{18}F]FDDNP$ ^{17,18} have been tested clinically and demonstrated potential utility for the diagnosis of AD. Conversely, more SPECT scanners have been installed for routine clinical imaging than PET imaging devices, which provides a certain advantage to the use of SPECT imaging agents. Therefore, SPECT is thought to be more valuable than PET in terms of routine diagnostic use. While the development of more useful $A\beta$ imaging probes for SPECT has been a critical issue, $[^{123}I]JIMPY$ is the only SPECT probe to be tested in humans.^{19–21} The preliminary clinical data for $[^{123}I]JIMPY$ showed a poor signal-to-noise ratio making it difficult to distinguish AD patients, possibly due to high lipophilicity and low stability.

Although many PET or SPECT imaging probes for cerebral $A\beta$ plaques have been reported, there has been no report on the development of dual imaging probes. To develop novel radiotracers offering both PET (^{18}F) and SPECT (^{123}I) imaging using a single compound, we designed a new candidate compound which has both fluoride and iodide in a single chemical structure. We have recently reported the use of radioiodinated aurone derivatives as a new backbone structure in the development of $A\beta$ imaging probes for SPECT.^{22,23} The derivatives showed strong binding to $A\beta$ aggregates, good penetration of the brain, and a fast washout from the brain despite their substituted groups. Among them, AR-1 (Fig. 1) showed the most promising characteristics as a SPECT probe in terms of affinity for $A\beta$ aggregates and radioactivity pharmacokinetics in the brain.

* Corresponding authors. Tel.: +81 75 753 4608; fax: +81 75 753 4568 (M.O.); tel./fax: +81 95 819 2441 (M.N.).

E-mail addresses: ono@pharm.kyoto-u.ac.jp (M. Ono), morio@nagasaki-u.ac.jp (M. Nakayama).

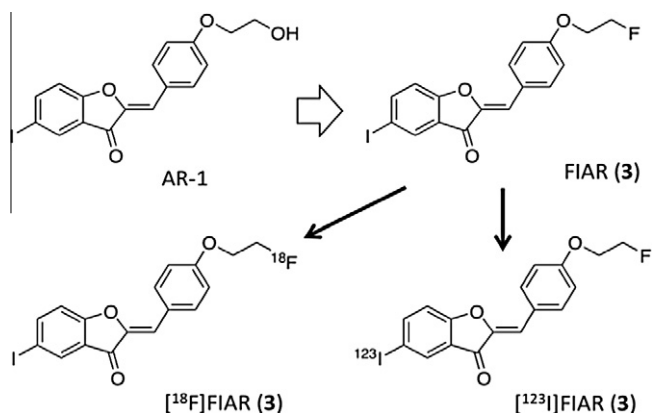


Figure 1. Flow chart of the development of PET/SPECT dual imaging probes for A β plaques.

In the present study, we designed and synthesized a new fluorinated and iodinated aurone derivative (FIAR) with a 2-fluoroethoxy group at the 4' position of AR-1 (Fig. 1) and evaluated its biological potential as a PET/SPECT dual imaging probe for A β by testing its affinity for A β aggregates in vitro and its uptake by and clearance from the brain in biodistribution experiments using normal mice.

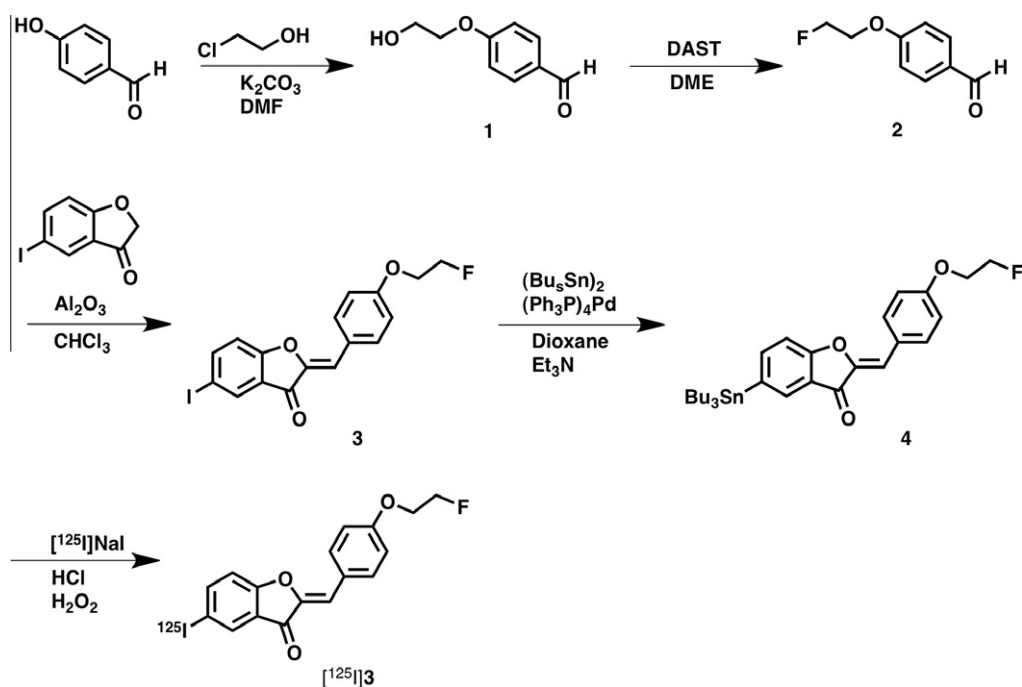
The target aurone derivatives were prepared as shown in Schemes 1 and 2. The synthesis of the aurone backbone was achieved by an Aldol reaction of benzofuranone with benzaldehyde using Al₂O₃.²⁴ In this process, 5-iodobenzofuran-3(2H)-one was reacted with 4-(2-fluoroethoxy)benzaldehyde **2** or 4-(2-hydroxyethoxy)benzaldehyde **1** in the presence of Al₂O₃ in chloroform at room temperature to form **3** and **5** in yields of 27% and 48%, respectively. The tributyltin derivative **4** was prepared from the corresponding compound **3** using a halogen to tributyltin exchange reaction catalyzed by Pd(0) for yields of 32.2%. The tributyltin derivative was used as the starting material for radioiodination in the preparation of [¹²⁵I]**3**. [¹²⁵I]**3** was achieved by an iododestannylation reaction using hydrogen peroxide as the oxidant, which produced the de-

sired radioiodinated ligand (Scheme 1). It was anticipated that the no-carrier-added preparation would result in a final product bearing a theoretical specific activity similar to that of ¹²⁵I (2200 Ci/mmol). The free OH groups of **5** were converted into tosylates by reacting with TsCl in the presence of pyridine to give **6**. To make the desired ¹⁸F-labeled aurone, [¹⁸F]**3**, the tosylate **6** was employed as the precursor. A solution of **6** in acetonitrile (200 μ L) was added to a reaction vessel containing ¹⁸F and the mixture was heated at 100 $^{\circ}$ C for 10 min (Scheme 2). The radiochemical identity of [¹²⁵I]**3** and [¹⁸F]**3** was verified by a comparison of retention times with the nonradioactive compound. These products were obtained in >23% radiochemical yields with a radiochemical purity of >95% after purification by HPLC.

In vitro binding experiments to evaluate the affinity of the aurone derivative **3** for A β aggregates were carried out in solution with [¹²⁵I]IMPY as the ligand. The compound inhibited the binding of [¹²⁵I]IMPY to A β (1–42) aggregates in a dose-dependent manner, indicating an affinity for A β aggregates (Fig. 2). The K_i value estimated for **3** was 6.81 nM. This value suggested that **3** had binding affinity sufficient for the in vivo imaging of A β (1–42) aggregates in the brain. The affinity was in the same range as that of aurone derivatives reported previously,^{22,23} indicating no decrease in binding even though the iodide and the fluoroethoxy group were both introduced into the aurone scaffold.

To confirm the affinity of aurone derivatives for A β plaques in the mouse brain, neuropathological staining with **3** was carried out using brain sections from transgenic mouse (Tg2576) (Fig. 3). Many A β plaques were clearly stained with **3**, as reflected by the high affinity for A β aggregates in inhibition assays in vitro (Fig. 3A). The labeling pattern of **3** was consistent with that of thioflavin-S, a dye commonly used for the detection of A β plaques (Fig. 3B), indicating that **3** has affinity for A β plaques in the mouse brain in addition to having binding affinity for synthetic A β 42 aggregates. Conversely, no apparent staining of **3** was observed in age-matched control mouse brain sections (Fig. 3C).

Furthermore, we investigated the affinity of [¹²⁵I]**3** for A β plaques by in vitro autoradiography in human AD brain sections (Fig. 4). The autoradiographic images of [¹²⁵I]**3** showed high levels



Scheme 1. Synthesis of [¹²⁵I]**3**.

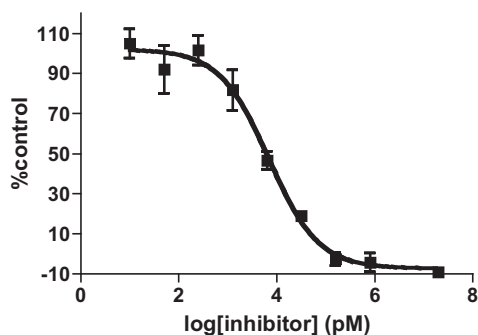
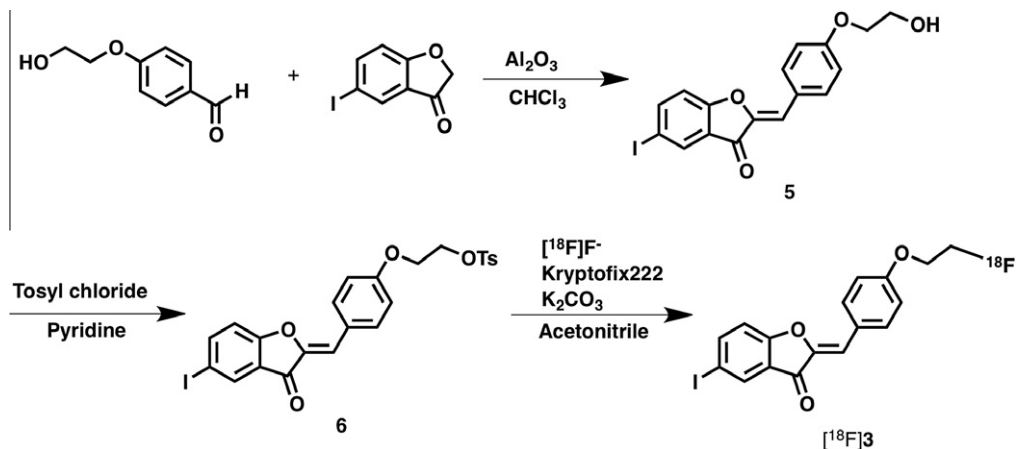


Figure 2. Competition curve for **3** against [¹²⁵I]IMPY.

of radioactivity in the brain sections (Fig. 4A). We confirmed that the hot spots of [¹²⁵I]**3** corresponded with those of in vitro

immunohistochemical staining (Fig. 4B). In contrast, normal human brain displayed no remarkable accumulation of [¹²⁵I]**3** (Fig. 4C). These results demonstrate the feasibility of using **3** as a probe for detecting A β plaques in the brains of AD patients by PET/SPECT.

The biodistribution of [¹²⁵I]**3** and [¹⁸F]**3** in vivo was tested in normal mice (Table 1). A biodistribution study provides important information on brain uptake. The ideal A β imaging probe should have good blood–brain barrier penetration to deliver a sufficient dose into the brain while achieving rapid clearance from normal regions to result in a higher signal-to-noise ratio in the AD brain. The initial brain uptake of [¹²⁵I]**3** was 2.34% of injected dose/gram at 2 min postinjection, whereas the radioactivity accumulated in the brain was rapidly eliminated (0.19% of injected dose/gram at 60 min postinjection), properties highly desirable for A β imaging probes. [¹⁸F]**3** displayed high uptake (3.66% of injected dose/gram at 2 min postinjection) into and rapid clearance (1.75% of injected

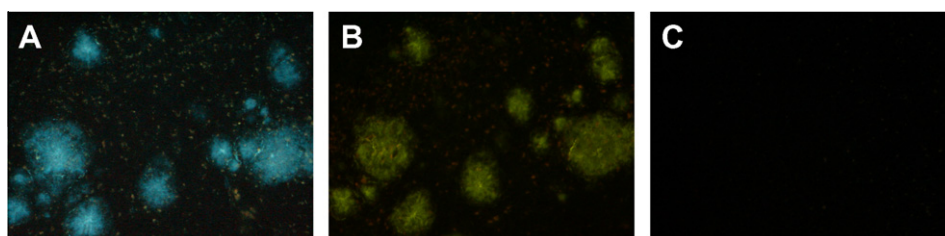


Figure 3. Fluorescent staining of **3** in 10- μ m Tg2576 mouse brain sections (A). Labeled plaques were confirmed by staining of the adjacent sections with thioflavin-S (B). No apparent staining of **3** was observed in the age-matched control mouse brain section (C).



Figure 4. In vitro ARG of [¹²⁵I]**3** revealed the distinct labeling of A β plaques in AD brain sections (A). The presence and localization of plaques in the sections were confirmed with immunohistochemical staining using a monoclonal β -amyloid antibody (B). Conversely, there was very little labeling of [¹²⁵I]**3** in a control brain section (C).

Table 1
Biodistribution of radioactivity after injection of [¹²⁵I]**3** and [¹⁸F]**3** in normal mice^a

Tissue	Time after injection (min)			
	2	10	30	60
[¹²⁵ I] 3 (log <i>P</i> = 2.45 ± 0.04) ^b				
Blood	6.70 (2.97)	3.13 (0.58)	1.94 (0.21)	1.29 (0.14)
Liver	17.06 (1.48)	16.50 (1.65)	12.44 (0.72)	10.96 (2.06)
Kidney	6.96 (0.76)	7.53 (0.85)	5.49 (1.21)	5.22 (1.95)
Intestine	2.02 (0.48)	6.53 (1.44)	12.35 (1.21)	15.74 (1.12)
Spleen	3.74 (0.48)	4.33 (0.87)	3.61 (0.85)	2.37 (0.59)
Pancreas	3.44 (0.58)	1.33 (0.33)	0.80 (0.16)	1.35 (0.09)
Heart	4.90 (0.86)	1.95 (0.26)	1.54 (0.22)	1.19 (0.53)
Stomach ^c	0.61 (0.07)	1.46 (1.85)	0.79 (0.51)	0.89 (0.35)
Brain	2.34 (0.36)	0.84 (0.23)	0.19 (0.03)	0.12 (0.06)
[¹⁸ F] 3				
Blood	5.72 (1.14)	2.84 (0.19)	2.68 (0.39)	2.61 (0.27)
Brain	3.66 (0.19)	2.37 (0.12)	1.77 (0.39)	1.75 (0.22)
Bone	2.03 (0.20)	2.13 (0.16)	3.45 (1.50)	3.42 (0.42)

^a Expressed as % injected dose per gram. Each value represents the mean (SD) for 5–6 animals.

^b Octanol/buffer (0.1 M phosphate-buffered saline, pH 7.4) partition coefficients. Each value represents the mean (SD) for three experiments.

^c Expressed as % injected dose per organ.

dose/gram at 60 min postinjection) from brain. [¹²⁵I]**3** and [¹⁸F]**3** showed different radioactivity pharmacokinetics in the brain despite of their similar chemical structure. This could be attributable to the difference in the physicochemical characteristics of their radiometabolites produced after injection of [¹²⁵I]**3** and [¹⁸F]**3** in vivo, but the precise reason remains unclear. However, data for **3** on radioactivity pharmacokinetics in the brain support the further development of dual probes for PET (¹⁸F) and SPECT (¹²³I) based on various Aβ-binding scaffolds using a single chemical structure.

In conclusion, we successfully designed and synthesized a fluorinated and iodinated aurone derivative as a probe for PET and SPECT to detect Aβ plaques in the brain. In binding experiments in vitro, **3** showed high affinity for Aβ aggregates. The aurone derivatives clearly stained Aβ plaques in an animal model of AD, reflecting their affinity for Aβ aggregates in vitro. In biodistribution experiments using normal mice, [¹²⁵I]**3** displayed good uptake in and fast washout from the brain. [¹⁸F]**3** also displayed high uptake in and good washout from brain, although a slight difference was observed between the ¹²⁵I and ¹⁸F tracers. A specific plaque labeling signal was clearly depicted by [¹²⁵I]**3** in postmortem AD brain sections. Taken together, the present results suggested that the fluorinated and iodinated aurone derivative may function as a PET/SPECT probe for detecting Aβ plaques in the AD brain.

Acknowledgments

The study was supported by the Funding Program for Next Generation World-Leading Researchers (NEXT Program), and a Grant-

in-aid for Young Scientists (A) and Exploratory Research from the Ministry of Education, Culture, Sports, Science and Technology, Japan.

Supplementary data

Supplementary data (procedure for the preparation of FIAR, in vitro binding assay, in vitro autoradiography using AD brain sections, and biodistribution studies) associated with this article can be found, in the online version, at doi:10.1016/j.bmcl.2011.08.063.

References and notes

- Klunk, W. E. *Neurobiol. Aging* **1998**, *19*, 145.
- Selkoe, D. J. *Physiol. Rev.* **2001**, *81*, 741.
- Selkoe, D. J. *Nat. Biotechnol.* **2000**, *18*, 823.
- Mathis, C. A.; Wang, Y.; Klunk, W. E. *Curr. Pharm. Des.* **2004**, *10*, 1469.
- Nordberg, A. *Lancet Neurol.* **2004**, *3*, 519.
- Kung, H. F.; Choi, S. R.; Qu, W.; Zhang, W.; Skovronsky, D. J. *Med. Chem.* **2010**, *53*, 933.
- Choi, S. R.; Golding, G.; Zhuang, Z.; Zhang, W.; Lim, N.; Hefti, F.; Benedum, T. E.; Kilbourn, M. R.; Skovronsky, D.; Kung, H. F. *J. Nucl. Med.* **2009**, *50*, 1887.
- Koole, M.; Lewis, D. M.; Buckley, C.; Nelissen, N.; Vandenbulcke, M.; Brooks, D. J.; Vandenberghe, R.; Van Laere, K. J. *Nucl. Med.* **2009**, *50*, 818.
- Zhang, W.; Oya, S.; Kung, M. P.; Hou, C.; Maier, D. L.; Kung, H. F. *Nucl. Med. Biol.* **2005**, *32*, 799.
- Rowe, C. C.; Ackerman, U.; Browne, W.; Mulligan, R.; Pike, K. L.; O'Keefe, G.; Tochon-Danguy, H.; Chan, G.; Berlangieri, S. U.; Jones, G.; Dickinson-Rowe, K. L.; Kung, H. P.; Zhang, W.; Kung, M. P.; Skovronsky, D.; Dyrks, T.; Holl, G.; Krause, S.; Friebe, M.; Lehman, L.; Lindemann, S.; Dinkelborg, L. M.; Masters, C. L.; Villemagne, V. L. *Lancet Neurol.* **2008**, *7*, 129.
- Johnson, A. E.; Jeppsson, F.; Sandell, J.; Wensbo, D.; Neelissen, J. A.; Jureus, A.; Strom, P.; Norman, H.; Farde, L.; Svensson, S. P. *J. Neurochem.* **2009**, *108*, 1177.
- Nyberg, S.; Jonhagen, M. E.; Cselenyi, Z.; Halldin, C.; Julin, P.; Olsson, H.; Freund-Levi, Y.; Andersson, J.; Varnas, K.; Svensson, S.; Farde, L. *Eur. J. Nucl. Med. Mol. Imaging* **2009**, *36*, 1859.
- Mathis, C. A.; Wang, Y.; Holt, D. P.; Huang, G. F.; Debnath, M. L.; Klunk, W. E. *J. Med. Chem.* **2003**, *46*, 2740.
- Klunk, W. E.; Engler, H.; Nordberg, A.; Wang, Y.; Blomqvist, G.; Holt, D. P.; Bergstrom, M.; Savitcheva, I.; Huang, G. F.; Estrada, S.; Ausen, B.; Debnath, M. L.; Barletta, J.; Price, J. C.; Sandell, J.; Lopresti, B. J.; Wall, A.; Koivisto, P.; Antoni, G.; Mathis, C. A.; Langstrom, B. *Ann. Neurol.* **2004**, *55*, 306.
- Ono, M.; Wilson, A.; Nobrega, J.; Westaway, D.; Verhoeff, P.; Zhuang, Z. P.; Kung, M. P.; Kung, H. F. *Nucl. Med. Biol.* **2003**, *30*, 565.
- Verhoeff, N. P.; Wilson, A. A.; Takeshita, S.; Trop, L.; Hussey, D.; Singh, K.; Kung, H. F.; Kung, M. P.; Houle, S. *Am. J. Geriatr. Psychiatry* **2004**, *12*, 584.
- Agdeppa, E. D.; Kepe, V.; Liu, J.; Flores-Torres, S.; Satyamurthy, N.; Petric, A.; Cole, G. M.; Small, G. W.; Huang, S. C.; Barrio, J. R. *J. Neurosci.* **2001**, *21*, RC189.
- Shoghi-Jadid, K.; Small, G. W.; Agdeppa, E. D.; Kepe, V.; Ercoli, L. M.; Siddarth, P.; Read, S.; Satyamurthy, N.; Petric, A.; Huang, S. C.; Barrio, J. R. *Am. J. Geriatr. Psychiatry* **2002**, *10*, 24.
- Kung, M. P.; Hou, C.; Zhuang, Z. P.; Zhang, B.; Skovronsky, D.; Trojanowski, J. Q.; Lee, V. M.; Kung, H. F. *Brain Res.* **2002**, *956*, 202.
- Zhuang, Z. P.; Kung, M. P.; Wilson, A.; Lee, C. W.; Plossl, K.; Hou, C.; Holtzman, D. M.; Kung, H. F. *J. Med. Chem.* **2003**, *46*, 237.
- Newberg, A. B.; Wintering, N. A.; Plossl, K.; Hochold, J.; Stabin, M. G.; Watson, M.; Skovronsky, D.; Clark, C. M.; Kung, M. P.; Kung, H. F. *J. Nucl. Med.* **2006**, *47*, 748.
- Ono, M.; Maya, Y.; Haratake, M.; Ito, K.; Mori, H.; Nakayama, M. *Biochem. Biophys. Res. Commun.* **2007**, *361*, 116.
- Maya, Y.; Ono, M.; Watanabe, H.; Haratake, M.; Saji, H.; Nakayama, M. *Bioconjugate Chem.* **2009**, *20*, 95.
- Bryant, W. M.; Huhn, G. F. *Synth. Commun.* **1995**, *25*, 915.